RSC Advances

This is an *Accepted Manuscript*, which has been through the Royal Society of Chemistry peer review process and has been accepted for publication.

Accepted Manuscripts are published online shortly after acceptance, before technical editing, formatting and proof reading. Using this free service, authors can make their results available to the community, in citable form, before we publish the edited article. This *Accepted Manuscript* will be replaced by the edited, formatted and paginated article as soon as this is available.

You can find more information about *Accepted Manuscripts* in the Information for Authors.

Please note that technical editing may introduce minor changes to the text and/or graphics, which may alter content. The journal's standard Terms & Conditions and the Ethical guidelines still apply. In no event shall the Royal Society of Chemistry be held responsible for any errors or omissions in this *Accepted Manuscript* or any consequences arising from the use of any information it contains.

ROYAL SOCIETY OF CHEMISTRY

www.rsc.org/advances

Cite this: DOI: 10.1039/c0xx00000x

www.rsc.org/xxxxxx

ARTICLE TYPE

Novel Conjugated Ag@PNIPAM Nanocomposites for Effective Antibacterial Wound Dressing

Shengping Gao,[a] Wei Ge,[a] Chunqiu Zhao,[a] Chuansheng Cheng,[a,b] Hui Jiang,[a] Xuemei Wang*[a]

Received (in XXX, XXX) Xth XXXXXXXXX 20XX, Accepted Xth XXXXXXXXX 20XX
DOI: 10.1039/b000000x

Abstract: It is well known that nanosilver or silver ions could act as an effective antibacterial agent without the development of bacterial resistance but long term exposure may induce *in vivo* toxicity. Thus, specific care should be taken before relevant silver-containing materials used as the antibacterial agents. Recently biocompatible polymeric materials are widely used to reduce toxic effects of nanomaterials, which could be utilized to fabricate antibacterial surface coatings with good biocompatibility. In this study we have developed a simple and green synthesis strategy to prepare Ag@PNIPAM nanocomposites with high purity and good bioactivity for promising bio-applications as highly effective antimicrobial agents. The relevant synthesis takes place in a clean environment without any chemical additives, which ensures ultrahigh active surfaces of the Ag clusters. The as-prepared Ag@PNIPAM nanocomposites exhibit highly effective antimicrobial activities against *Staphylococcus aureus* (*S. aureus*) and have a good therapeutic effect for burn wounds.

1. Introduction

Resistance of bacteria to bactericides and antibiotics has attracted much attention in recent years due to the development of resistant strains which is the main obstacle for the effective treatment[1, 2]. Some antimicrobial agents are extremely irritant and toxic so that much effort has been explored to design or formulate new types of safe and cost-effective bactericidal materials, which may strongly resist bacterial adhesion or kill bacteria and prevent biofilm formation[3-6]. These antibacterial materials should be biocompatible and bioactive with high-performance for bactericidal action[7]. Some noble metal materials, especially relevant nanomaterials including gold or silver nanoparticles, which can readily get attached to the bacterial membrane and disrupt its integrity, have attracted increasing attention in the field of biomedicine as promising antimicrobial agents[8, 9]. In particular, silver has been shown to enhance regeneration of soft tissue such as skin, and nanosilver has been found to be one of the most promising antibacterial nanomaterials, which can effectively inhibit bacterial resistance and execute much more efficient antibacterial action as compared to bulk silver materials[10]. Recent development of bio-nanotechnology has facilitated the production of biocompatible silver nanoparticles with increasingly large surface area-to-volume ratios, with greater efficacy for bactericidal action and lower toxicity to environment and human beings[11-13]. Ag nanoparticles with size smaller than 2 nm, known as Ag nanoclusters, consisting of a few to several hundred metal atoms, have received much attention in recent years due to their ultrasmall size, and a large bioactive surface area. Thus, these nanoclusters could be readily introduced on a surface coating to greatly enhance the relevant bactericidal activity[14-16]. However, it is still illusive to fabricate broad antibacterial surface coatings with strong bactericidal effects and good biocompatibility/environmental safety by using Ag clusters[17, 18].

It is already known that the aggregation of Ag clusters, uncontrollable release of silver ions and promoted adhesion of bacteria can greatly reduce antibacterial efficacy of Ag nanoparticles. Undoubtedly, aggregation of Ag clusters can readily decrease contact possibility of bacteria and nanoparticles. Therefore, highly dispersed Ag clusters is desirable for the formation of effective antibacterial agents[19, 20], though it is still very hard to find a convenient synthesis approach to produce these antibacterial material with optimized properties. Based on the above consideration, we have explored the possibility to control the size, shape, surface properties, and aggregation degree of nanosilver for realizing good performance of antibacterial action. And the biocompatible polymers have been explored to combine with nanosilver to control silver ions release, surface charge, dispersion status and even the shape of nanosilver for achieving desirable bioactive and antibacterial effects[21].

Poly (N-isopropylacrylamide) (PNIPAM) is one of the most widely studied and environmentally responsive polymers owing to its thermo-sensitivity, biocompatibility and great structure tailorability and flexibility[22]. In aqueous solution, PNIPAM undergoes a phase transition from a hydrophilic state to a hydrophobic state as the temperature is raised above the lower critical solution temperature (LCST), which is about 32 ℃[23]. The PNIPAM nanomaterials can readily inhibit relevant aggregation and form uniform surface coatings on various substrates[24], and thus be capable of controlling the release of silver ions for

RSC Advances Accepted Manuscript

sustained antibacterial effects and reduce cytotoxicity[25]. More importantly, they can be designed to resist bacteria adhesion and enhance bactericidal properties[4]. Thus, it is possible to combine Ag cluster and PNIPAM polymer matrix to form multifunctional nanocomposite coatings for promising antibacterial applications[26, 27]. In order to improve the antibacterial activity of Ag clusters, there are significant challenges in synthesizing bioactive Ag cluster with ultrahigh surface activity. In this contribution, we have developed a simple and green approach to synthesize highly pure, well-crystalline and smooth-surfaced Ag@PNIPAM with highly effective bioactive and antimicrobial activities. The relevant synthesis takes place in a clean and slow reaction environment without any chemical additives, which ensures ultrahigh active surfaces of the Ag clusters owing to their ultrasmall size. The as-prepared Ag@PNIPAM exhibit highly effective antimicrobial activities against *Staphylococcus aureus* and have an efficient therapeutic effect for burn wounds.

2. Experimental Section

2.1. Materials

Silver nitrate ($AgNO_3$, 99.95%, metals basis, Ag 63% min), $(NH_4)_2S_2O_8$ (APS) and $Na_2S_2O_5$ (SPS) were purchased from Shanghai Chemical Reagents Company and used without further purification. Glutathione (GSH), N, N'-methylenebisacrylamide (MBA) and N-isopropylacrylamide (NIPAM) were purchased from Sigma Aldrich. *Staphylococcus aureus* (*S. aureus*, Gram-positive bacteria) strains were provided by the first affiliated hospital of Dalian medical university (Dalian, China). The ultrapure water (Millipore, 18.2 MΩ cm) was used to prepare solutions. The phosphate buffer solution (PBS, 0.1 M, pH 7.4) was prepared by using double distilled water (Millipore Ltd., USA). All solutions were stored in the refrigerator at 4 ℃.

2.2. Preparation of Ag@PNIPAM nanocomposite

The polymer of the Ag@PNIPAM nanocomposite was synthesized through a free radical polymerization by two steps (Scheme 1). Initially, 0.5g NIPAM and 15.0mg MBA were dissolved in 15 mL water, and then 11mg APS and 9 mg SPS was separately dissolved in 1.5 mL water. The NIPAM aqueous solution and MBA aqueous solution were added into flask under nitrogen at 50-60 ℃. After 30 min, the polymerization was initiated by the injection of APS and SPS aqueous solution. It is noted that after a few minutes the solution color changed from the transparent to light blue, and then slowly turned to milky white. The reaction was allowed to proceed at 60 ℃ for 6 h. In order to remove some oligomers and unreacted monomers, the obtained polymer dispersion was diluted with water, then purified by dialysis for about 7 days, and finally redispersed in water for further experiments.

Afterwards, 1 mL of $AgNO_3$ aqueous solution (34 μg/mL) was freshly prepared and used for the synthesis of Ag NCs. 1 mL of GSH aqueous solution (38 μg/mL) was added dropwise into the $AgNO_3$ solution and let to react with silver ions until it became clear. The bulky molecular structure of GSH as the ligand could play a critical role in the gelation with Ag^+ ions, leading to the formation of the relevant stable hydrogel complex.[11] The complex mixture was added into PNIPAM mixture and incubated at 30 ℃ about 7 days. The product was diluted with water (15 mL) and washed three times by centrifugation (30 min, 8000 rpm) and redispersion in water (5 mL). At last, thermo-sensitive Ag@PNIPAM nanocomposites could be readily obtained.

2.3. Characterization of Ag@PNIPAM Nanocomposites

The size and morphology of the as-prepared Ag NCs and Ag@PNIPAM were examined by transmission electron microscopy (TEM). The TEM images were obtained by using a Hitachi H-600 transmission electron microscope operating at 100 kV. The scanning electron microscopic (SEM) images were obtained on an ultra plus field emission SEM (Zeiss, Germany), with an acceleration potential at 10 kV. After critical point drying, a small amount of gold was sputtered on the samples to avoid charging in the microscope. The crystalline phase was determined by powder X-ray diffraction (XRD) pattern (Bruker D8, Cu–Ka radiation) obtained on a DMAX-B (Rigaku Denki Corp., Tokyo, Japan). The UV-Vis absorption spectra was performed on HITACHI U-4100 ultraviolet spectrophotometer.

2.4. Cytotoxicity assay by MTT method

A549 lung cancer cells were seeded into 96-well plates at an intensity of 7×10^4 cells mL^{-1} and maintained for 24 h in DMEM medium (Gibco, USA) Different amounts of Ag@PNIPAM nanocomposites with a concentration of 0.5 μM were then added into the medium, and the cells were incubated in the DMEM for different time (12, 24, 36, 48 and 72 h) at 37 ℃. After pouring out the medium, 100 mL of freshly prepared MTT (1 mg mL^{-1} in PBS) was added to each well and incubated for 4 h. After removing the MTT medium solution, the cells were lysed by adding 150 mL of DMSO. The plate was gently shaken for 5 min, and then the absorbance of purple formazan at 520 nm was monitored by using a Spectra MAX340PC plate reader[28]. In order to provide a comparative study of the toxicity of nanoparticles to the cells, bare Ag NCs and PNIPAM were also added instead of the Ag@PNIPAM nanocomposites to incubate with the cells in the MTT experiment. The amount of the nanoparticles remained the same as the Ag@PNIPAM nanocomposites.

2.5. Bacterial testing of growth curve and antibacterial activity of nanocomposites

To examine the bacterial growth rate in the presence of different antibiotics, *S. aureus* strains were grown in 100 ml of liquid Luriae-Bertani (LB) broth medium supplemented with 5×10^6 CFU of *S. aureus* cells in 1.5mg/mL PNIPAM, 15 μg/mL Ag NCs or 15 μg/mL Ag@PNIPAM (the concentration of Ag NCs) respectively. Growth rates and bacterial concentrations were determined by measuring optical density (OD) at 600 nm. Then the OD values were used to calculate the concentration of *S. aureus* strains.

The zone of inhibition test was employed to evaluate the synergistic effects between Ag NCs and the PNIPAM. The bacteria were incubated in LB broth at 37 ℃ overnight. The resulting bacterial suspension was diluted to approximate 1.0×10^7

RSC Advances Accepted Manuscript

This journal is © The Royal Society of Chemistry [year]

CFU/mL with LB broth. Subsequently, 50 mL of the bacterial suspension were inoculated evenly on LB agar plates. Then, the sample disk containing the antimicrobial agent solution was gently placed at the center of the LB agar plates and incubated overnight at 37 ℃. The antibacterial activity was measured by evaluating the diameter of the zone of inhibition around the disk. Statistical analysis was conducted on the experimental results.

2.6. Established mouse model of burn wound

We use a scalding device of electrical heating, the temperature can reach 200 ℃. Wounds were burned by this device in mice back surface of the rear side perpendicular to the skin. The wounds showed a circular area of about 4.0 cm^2 (diameter about 1.1 cm), which is identified as superficial Ⅱ degree burns. All experiments involving mice were approved by the National Institute of Biological Science and Animal Care Research Advisory Committee of Southeast University, and the burn wound procedure was conducted following the guidelines of the Animal Research Ethics Board of Southeast University.

2.7. Animal experiments of antibacterial activity

Animal experiments were reviewed, approved, and supervised by the Jiangsu province Institutional Animal Care and Use Committee of China. Pathogen-free 8-week-old male Kunming mice (i.e. Swiss mice), of clean grade, weighing from 28 to 32 g, were obtained from Qinglongshan animal farm of Nanjing and were maintained in high efficiency particulate air-filtered barrier units kept inside biological safety cabinets for the duration of the experiments. Mice were given free access to tap water and pelleted rodent food and were kept at 25 ℃ with alternating 12 h periods of light and dark. Animals were randomly assigned to three groups (unless otherwise noted), i.e., control group, treated with Ag NCs group and treated with Ag@PNIPAM group.

Before using, bacteria were grown in LB broth medium, centrifuged at 5000 rpm for 5 min, washed and suspended in sterile PBS, and maintained at 37 ℃. Animals were clearly moribund or on the verge of death were killed with an overdose of pentobarbital sodium (150 mg/kg).

Ten microliters of bacterial solution (1.8×10^5 CFU/cm^2 *S. aureus*) were applied topically to each wound and were allowed to absorb for 15 minutes. Wounds were covered and monitored. Preparation of Ag@PNIPAM onto the wound contact surface of Ag was performed. Wounds were created and splinted as described earlier. Control mice were untreated with nanocomposites and the experimental group received treated with Ag NCs or Ag@PNIPAM.

2.7. Statistics

All experiments were conducted in triplicate, and data points were expressed as the mean. F-test was used for significance testing, and $p<0.05$ is considered to be statistically significant.

3. Results and Discussion

3.1. Characterization of Ag@PNIPAM Nanocomposites

Figure 1a shows the TEM micrographs of Ag@PNIPAM nanocomposites. It can be established that synthesized Ag NCs involved silver atoms planes with an interplanar distance of ca. 0.1 nm, were almost spherical and had no noticeable trend to agglomerate. Such a narrow size distribution and the absence of agglomeration suggest that the reduction of silver ions into Ag clusters occurs through the involvement of self-assembling reducing ligand(s), which leads to simultaneously facilitate the reduction course by Ag(0) coordination (viz., decreasing the reduction potential of Ag^+ by decreasing the thermodynamic requirement through stabilizing Ag(0) clusters and facilitating kinetics by avoiding that the reaction proceeds through naked Ag(0) atoms) and effectively tailor the surface of growing Ag NCs. Scanning electron microscope (SEM) images of Ag@PNIPAM were shown in Figure 1b. The shape of these Ag@PNIPAM nanocomposites was close to being spherical and the average diameter was about 100 nm. It is easy to notice that most of Ag NCs uniformly. X-ray diffraction (XRD) measurements confirm the structure of Ag@PNIPAM and PNIPAM. Fig. 1c shows diffraction peak at 2θ=7.56 and 21.97, which corresponds to the amorphous phase of the PNIPAM[29]. The diffraction peak at 2θ=38.12, 44.27, 64.43, 77.47 81.54, which distinct reflections observed for the compounds were (111), (200), (220), (311), (222), commonly used for the description of Ag cluster structures[30, 31.] The Ag@PNIPAM and PNIPAM were characterized by UV-Vis absorption spectroscopy, (Fig.1d) confirming that Ag nanoclusters connect with PNIPAM.

3.2 Cytotoxic effect of Ag@PNIPAM on A549 cells

The cytotoxicity of the carriers in the drug-delivery system has been also investigated in this study. Initially, the cytotoxicity effect of Ag cluster, PNIPAM and Ag@PNIPAM on A549 cells were all characterized by MTT. Fig. 2 shows cell viabilities against Ag cluster, PNIPAM and Ag@PNIPAM with different concentration. The results demonstrate that the cytotoxic efficacy of the Ag@PNIPAM and free Ag cluster increases with the increasing Ag concentrations, and the Ag@PNIPAM exhibit significantly lower cytotoxicity than free Ag cluster. Meanwhile, it can be seen from the cell viability study in Fig. 2 that PNIPAM alone did not have a significant effect in cell viabilities after 48 h of incubation, indicating that PNIPAM have relatively low cytotoxicity. This raises the possibility for the PNIPAM to be utilized as promising candidates for potential drug loading and delivery for antibacterial. This may be attributed to control the release of Ag by PNIPAM after adhesion to A549 cells[32, 33].

3.3 *In vitro* Antimicrobial Activity of Ag@PNIPAM

The growth curves of *S. aureus* in LB medium with 5.0×10^6 CFU with PNIPAM, Ag NCs, and Ag@PNIPAM are shown in Fig. 3. The dynamics of bacterial growth was also monitored in liquid LB medium supplemented with 5×10^6 CFU of *S. aureus* cells in 1.5 mg/mL PNIPAM, 15 μg/mL Ag NCs or 15 μg/mL Ag@PNIPAM (the concentration of Ag NCs). In Fig. 3a, PNIPAM of 1.5 mg/mL caused no obvious effect of growth of *S. aureus* and 15 μg/mL Ag NCs induced a little delay of exponential growth and stationary phase. Comparatively, Ag@PNIPAM not only greatly delays the exponential phase but also decreases the duration of the growth exponential phase. The growth transitions quickly from the exponential phase to a very low stationary phase. The test of the bacterial dynamics confirms

RSC Advances Accepted Manuscript

that Ag@PNIPAM results in a greater bactericidal effect on *S. aureus* cells than Ag NCs of the antibacterial reagents applied alone. This experiment provided solid evidence of the synergistic antibacterial effect of Ag@PNIPAM. Moreover, the quantitative inhibition abilities of agent was performed in order to delineate the changes of *S. aureus* treated with different concentration. The inhibition abilities of the separate PNIPAM, Ag NCs solution or the Ag@PNIPAM hydrogel solution are shown in Figure 3b. The full inhibition abilities were attained at 25 µg/mL silver for Ag@PNIPAM hydrogel solution and 60 µg/mL silver for the Ag NCs solution. It is noted that the Ag@PNIPAM hydrogel solution exhibited higher inhibitory activity than the Ag NCs solution at the same concentration of silver. Thus, *S. aureus* with different treartment concentration of Ag NCs solution and Ag@PNIPAM hydrogel solution indicates that Ag@PNIPAM hydrogel exhibits better inhibitory effect than Ag NCs[34].

In addition, the zone of the inhibition test was also performed to determine the synergistic effects between Ag NCs and PNIPAM. For this purpose, Ag NCs and Ag@PNIPAM at a final concentration of silver of 30 µg/mL, respectively, was prepared. As shown in Fig. 4, the diameters of zone of inhibition of Ag@PNIPAM were comparable with those of the Ag NCs, suggesting that Ag@PNIPAM exhibited most effective antimicrobial performance. Moreover, lower doses of Ag@PNIPAM were found to reduce the toxicity of Ag NCs. The synergistic effect not only enhanced the antimicrobial activity against multiple bacteria, but also prevented the emergence of bacterial resistance[35].

3.4 Wound Infection with *S. aureus*

In vivo Studies of Antibacterial Assay with Ag@PNIPAM

All mice were involved in the relevant in vivo studies with no mortality, surgical complications, and signs of pain, illness, or significant weight loss. Wounds without treatment of bacteria (control group) had minimal growth of organisms on day 1 and 2 and significant bacterial infections and wound area increases by day 3 and 4. *S. aureus* infection in the wound, respectively. To compare, the significant improvement could be observed after Ag and Ag@PNIPAM treatment for 7 days, as shown in Fig. 5. As can be seen in Figure 5 (b1), the wound treated with Ag NCs was deteriorated; in comparison, the wound treated with Ag@PNIPAM tends to heal and scar (see Figure 5 (c1)). These observations indicate that Ag@PNIPAM has highly effective antibacterial activity and could facilitate the repairing effect of dermal tissue and also promote the relavant wound healing. From the above observations, it is evident that Ag@PNIPAM has effective antibacterial activity. To examine the status of wound healing and the effect of dermal tissue after administration of Ag@PNIPAM, histological evaluation of rat dermal wound was performed at the 7th day after treatment. Representative hematoxylin and eosin (H&E)-stained histological images are shown in Fig. 6. Epithelialization, formation of granulation tissue, and contraction of underlying wound connective tissues can be observed in Fig. 6, indicating the efficient wound healing. However, in control studies, as shown in Fig. 6a and b, massive inflammatory cells can still be observed at the wound site due to wound infection without perfect repairing. These results showed that Ag@PNIPAM has highly effective antibacterial activity not only on repairing effect of dermal tissue, but also on the promoted wound healing.

Inserting Graphics

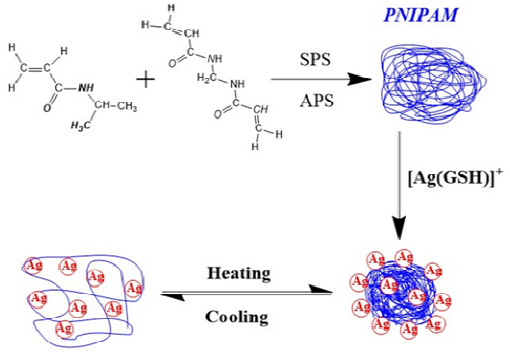

Scheme 1. Schematic illustration of the synthesis process of conjugated polymer Ag@PNIPAM nanocomposites.

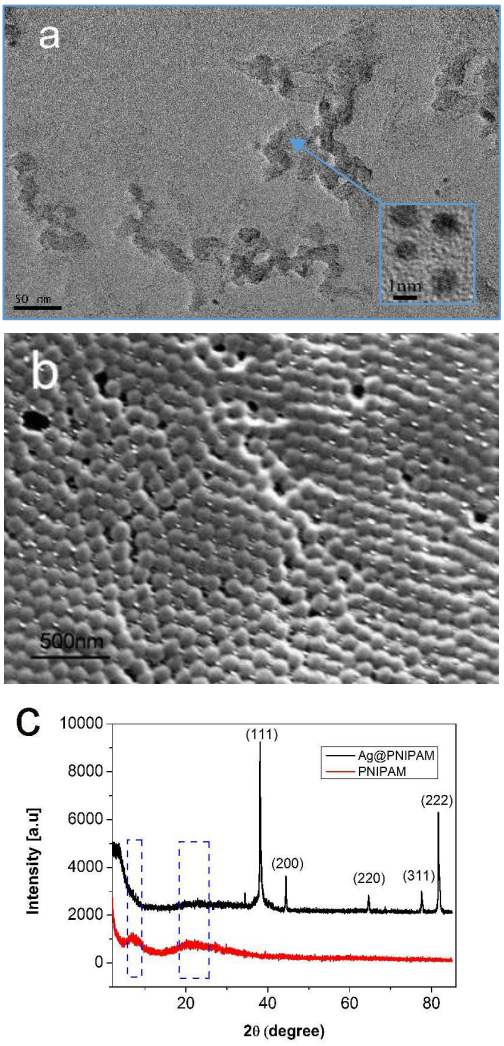

RSC Advances Accepted Manuscript

This journal is © The Royal Society of Chemistry [year]

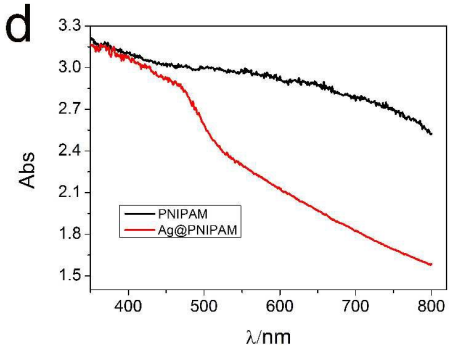

Fig.1. Characterization of Ag@PNIPAM. a): TEM image of the synthesized Ag@PNIPAM nanocomposites, evidencing the ~0.1 nm interplanar spacing of the silver nanoclusters (inset). b): SEM image of the Ag@PNIPAM. c): The powder X-ray diffraction patterns of Ag@PNIPAM and PNIPAM. d): UV-Vis absorption spectrum of the Ag@PNIPAM and PNIPAM.

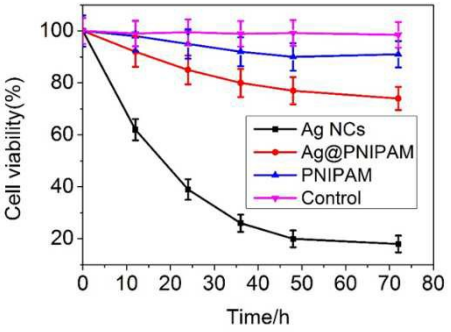

Fig.2. MTT assay assessment of time-dependent cytotoxicity activities of Ag NCs, Ag@PNIPAM and PNIPAM towards A549 cells for different incubation times. Fluorescence excitation wavelength is 590 nm. Data were expressed as the means ± SD (standard deviation) from at least three independent experiments.

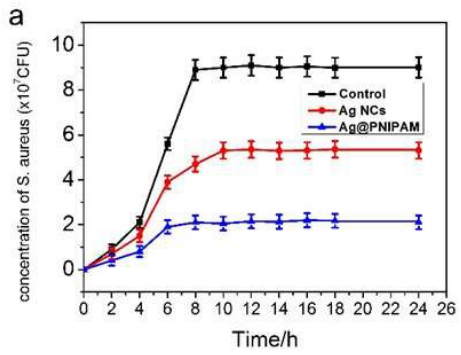

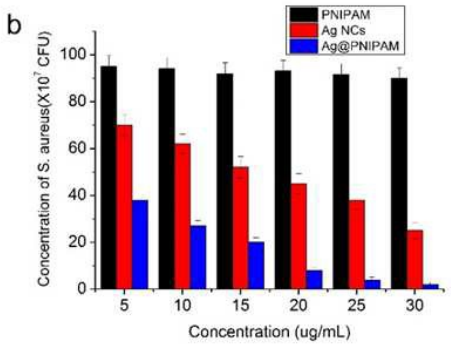

Fig.3. a): Growth curve of *S. aureus* in LB medium with 5.0×10^6 CFU without any antimicrobial agent (with PNIPAM) and in the presence of Ag NCs and the combination of Ag NCs and PNIPAM. b): Quantitative results of inhibition abilities of agent was performed in order to delineate the changes of *S. aureus* treated with different incubation concentration

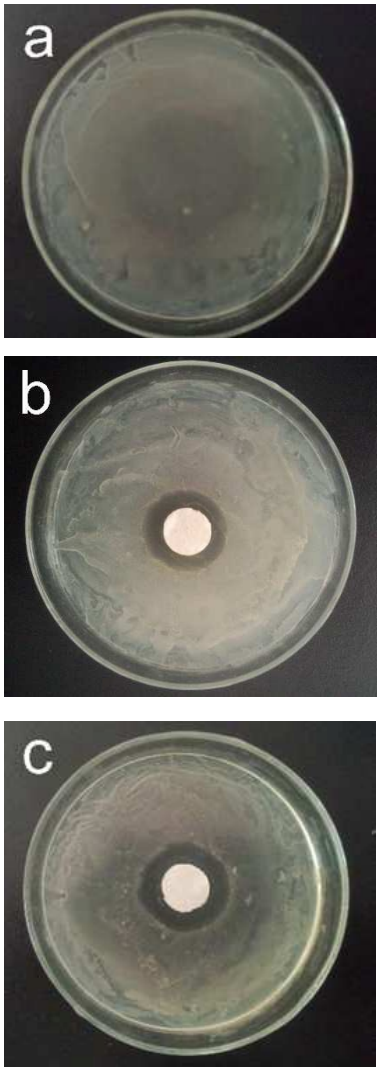

Fig.4. Bacterial inhibition zones of Ag NCs and Ag@PNIPAM. a): treated with PNIPAM, b): treated with Ag NCs, c: treated with Ag@PNIPAM.

RSC Advances Accepted Manuscript

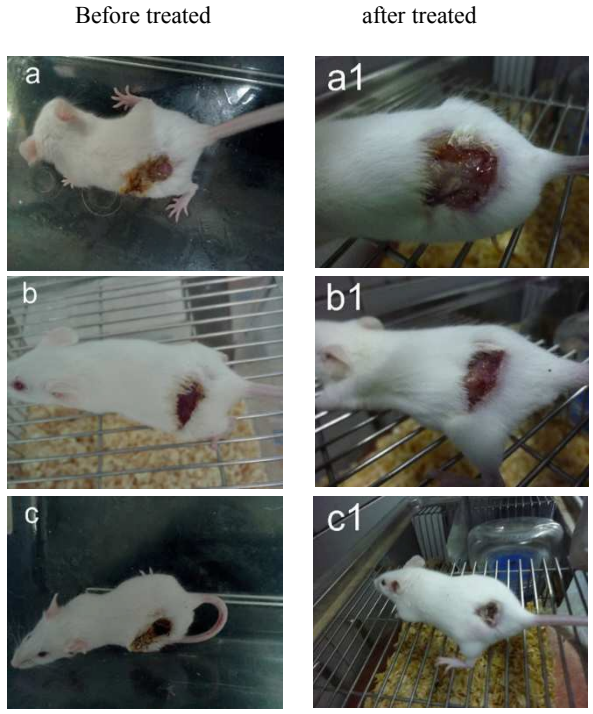

Fig.5. Wound healing effect of rat skin after relevant treatment for 7 days. a) and a1): control group (or treated with PNIPAM); b) and b1): treated with Ag NCs; c) and c1): treated with Ag@PNIPAM.

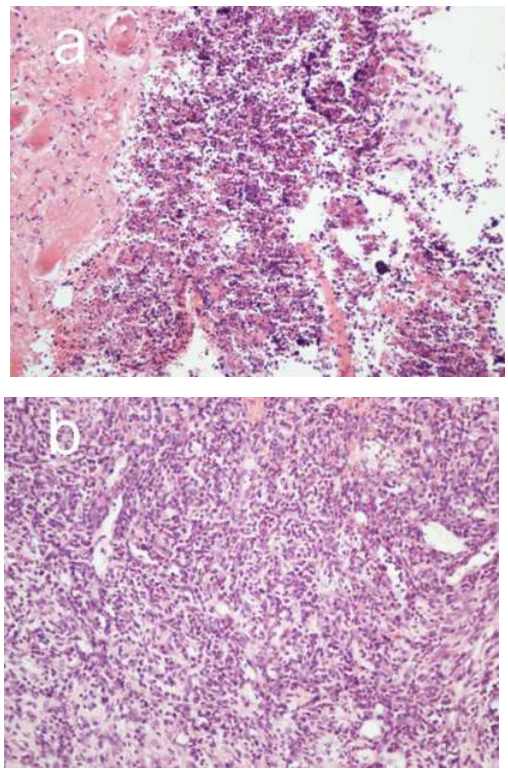

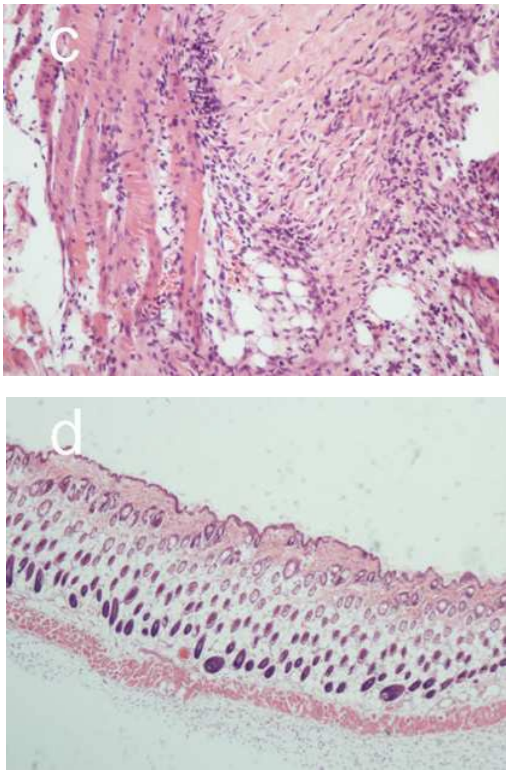

Fig.6. H&E staining of rat skin after treatment for 7 days. a): treated with PNIPAM; b): treated with Ag NCs; c): treated with Ag@PNIPAM; d): blank control group.

4. Conclusions

In summary, in this study we have developed a simple and green synthesis strategy to prepare Ag@PNIPAM nanocomposites with high purity, good crystallinity and smooth surfaces for promising bio-applications as highly effective antimicrobial agents. The Ag@PNIPAM nanocomposites were synthesized through fast reduction of silver ions in a solution of silver nitrate and GSH. The GSH used here is a natural compound and acts as a very good chelating and reducing agent; and the as-prepared Ag@PNIPAM nanocomposites demonstrate much more effective antimicrobial activity for bacteria like *S. aureus* than that of Ag NCs alone[36]. This raises the possibility to utilize the relevant Ag@PNIPAM nanocomposites as the promising new antibacterial agents or antimicrobial packaging materials for efficient wound dressings.

Notes

[*a] *State Key Lab of Bioelectronics (Chien-Shiung WU Laboratory), Southeast University, Nanjing 210096, P. R. China;*
[*b] *School of Chemistry and Chemical Engineering, Southeast University, Nanjing 211189, China; E-mail: xuewang@seu.edu.cn*

Acknowledgments

This work is supported by the National Natural Science Foundation of China (81325011), National High Technology Research & Development Program of China (2012AA022703), National Basic Research Program (2010CB732404), and the Major Science & Technology Project of Suzhou (ZXY2012028).

RSC Advances Accepted Manuscript

This journal is © The Royal Society of Chemistry [year]

References

1. F. Allerberger, A. Lechner, A. Wechsler-Fordos, R. Gareis and A. Int, *Chemotherapy*, 2008, **54**, 260-267.
2. D. Archana, B. K. Singh, J. Dutta and P. K. Dutta, *Carbohydr Polym*, 2013, **95**, 530-539.
3. B. Liu, S. Q. Shen, J. W. Luo, X. Y. Wang and R. C. Sun, *Rsc Adv*, 2013, **3**, 9714-9722.
4. S. H. Li, Z. J. Wang, Y. F. Wei, C. Y. Wu, S. P. Gao, H. Jiang, X. Q. Zhao, H. Yan and X. M. Wang, *Biomaterials*, 2013, **34**, 902-911.
5. S. H. Li, C. Y. Wu, X. Tang, S. P. Gao, X. Q. Zhao, H. Yan and X. M. Wang, *Sci China Chem*, 2013, **56**, 595-603.
6. K. Y. Choi, G. Liu, S. Lee and X. Y. Chen, *Nanoscale*, 2012, **4**, 330-342.
7. Y. Chen, L. D. Yan, T. Yuan, Q. Y. Zhang and H. J. Fan, *J Appl Polym Sci*, 2011, **119**, 1532-1541.
8. R. Hu, G. Z. Li, Y. J. Jiang, Y. Zhang, J. J. Zou, L. Wang and X. W. Zhang, *Langmuir*, 2013, **29**, 3773-3779.
9. D. Archana, J. Dutta and P. K. Dutta, *Int J Biol Macromol*, 2013, **57**, 193-203.
10. F. A. Sheikh, N. A. M. Barakat, M. A. Kanjwal, S. H. Jeon, H. S. Kang and H. Y. Kim, *J Appl Polym Sci*, 2010, **115**, 3189-3198.
11. S. Gao, D. Chen, Q. Li, J. Ye, H. Jiang, C. Amatore and X. Wang, *Scientific reports*, 2014, **4**, 4384.
12. S. H. Li, S. P. Gao, C. Y. Wu, J. L. Wang, H. Jiang and X. M. Wang, *Nanosci Nanotech Let*, 2013, **5**, 228-231.
13. S. Y. Zhang, J. W. Liu, C. L. Zhang and S. H. Yu, *Nanoscale*, 2013, **5**, 4223-4229.
14. H. Amiri, M. Mahmoudi and A. Lascialfari, *Nanoscale*, 2011, **3**, 1022-1030.
15. Z. P. Sun, Y. L. Wang, Y. T. Wei, R. Liu, H. R. Zhu, Y. Y. Cui, Y. L. Zhao and X. Y. Gao, *Chem Commun*, 2011, **47**, 11960-11962.
16. H. Y. Yang, Y. Wang and N. F. Zheng, *Nanoscale*, 2013, **5**, 2674-2677.
17. M. Benelmekki, M. Torrell, E. Xuriguera, F. Vaz and V. Teixeira, *Journal of Nano Research*, 2012, **18-19**, 105-116.
18. T. T. Zhao, Q. Y. Chen, P. D. Wang and Z. P. Chen, *Rsc Adv*, 2014, **4**, 10390-10394.
19. Z. H. Wei, Z. J. Zhou, M. Yang, C. H. Lin, Z. H. Zhao, D. T. Huang, Z. Chen and J. H. Gao, *J Mater Chem*, 2011, **21**, 16344-16348.
20. I. Diez and R. H. A. Ras, *Nanoscale*, 2011, **3**, 1963-1970.
21. P. Luo, S. N. Wang, T. T. Zhao and Y. Li, *Rare Metals*, 2013, **32**, 113-121.
22. H. Vihola, A. Laukkanen, L. Valtola, H. Tenhu and J. Hirvonen, *Biomaterials*, 2005, **26**, 3055-3064.
23. X. Zhu, C. Yan, F. M. Winnik and D. Leckband, *Langmuir*, 2007, **23**, 162-169.
24. Y. P. Zhang, K. Liu, Y. Guan and Y. J. Zhang, *Rsc Adv*, 2012, **2**, 4768-4776.
25. S. R. Deka, A. Quarta, R. Di Corato, A. Riedinger, R. Cingolani and T. Pellegrino, *Nanoscale*, 2011, **3**, 619-629.
26. H. J. Yoo and H. D. Kim, *J Appl Polym Sci*, 2008, **107**, 331-338.
27. G. M. Nisola, J. S. Park, A. B. Beltran and W. J. Chung, *Rsc Adv*, 2012, **2**, 2439-2448.
28. S. Gao, C. Wu, H. Jiang, D. Chen, Q. Li, X. Liu and X. Wang, *Rsc Adv*, 2014, **4**, 20841.
29. A. GhavamiNejad, S. Hashmi, H. I. Joh, S. Lee, Y. S. Lee, M. Vatankhah-Varnoosfaderani and F. J. Stadler, *Phys Chem Chem Phys*, 2014, **16**, 8675-8685.
30. Y. Murali Mohan, K. Lee, T. Premkumar and K. E. Geckeler, *Polymer*, 2007, **48**, 158-164.
31. Y. M. Mohan, T. Premkumar, K. Lee and K. E. Geckeler, *Macromol Rapid Comm*, 2006, **27**, 1346-1354.
32. X. Bai, S. Sandukas, M. Appleford, J. L. Ong and A. Rabiei, *Journal of Biomedical Materials Research Part B-Applied Biomaterials*, 2012, **100B**, 553-561.
33. X. P. Li, S. L. Li, M. T. Zhang, W. L. Zhang and C. H. Li, *Rare Metal Mat Eng*, 2011, **40**, 209-214.
34. A. M. Youssef and M. S. Abdel-Aziz, *Polym-Plast Technol*, 2013, **52**, 607-613.
35. S. Calderon, R. E. Galindo, J. C. Oliveira, A. Cavaleiro and S. Carvalho, *Surf Coat Tech*, 2013, **222**, 104-111.
36. I. A. Shurygina, B. G. Sukhov, T. V. Fadeeva, V. A. Umanets, M. G. Shurygin, T. V. Ganenko, Y. A. Kostyro, E. G. Grigoriev and B. A. Trofimov, *Nanomed-Nanotechnol*, 2011, **7**, 827-833.

RSC Advances Accepted Manuscript